Mathematics

https://www.aimspress.com/journal/Math

AIMS Mathematics, 10(1): 584–597.
DOI: 10.3934/math.2025026
Received: 26 November 2024
Revised: 23 December 2024
Accepted: 27 December 2024
Published: 10 January 2025

Research article

Exponential stability of ARZ traffic flow model based on 2×2 variable-coefficient hyperbolic system

Yiyan Wang[1], **Dongxia Zhao**[1,*], **Caifen Sun**[1] **and Yaping Guo**[2]

[1] School of Mathematics, North University of China, Taiyuan 030051, China
[2] School of Mathematical Sciences, Shanxi University, Taiyuan 030006, China

* **Correspondence:** Email: zhaodongxia6@sina.com.

Abstract: This paper studies the exponential stability of the Aw-Rascle-Zhang (ARZ) traffic flow model. Given that the steady state may be non-uniform, we obtain a 2×2 hyperbolic system with variable coefficients. Then, by combining ramp metering and variable speed limit control, we deduce a kind of proportional boundary feedback controller. The well-posedness of the closed-loop system is proved by using the theory of semigroups of operators. Moreover, a novel Lyapunov function, whose weighted function is constructed by the solution of a first-order ordinary differential equation, can be used for the stability analysis. The analysis gives a sufficient stability condition for the feedback parameters, which is easy to verify. Finally, the effectiveness of boundary control and the feasibility of the feedback parameters are obtained by numerical simulation.

Keywords: boundary feedback control; exponential stability; Lyapunov function; traffic flow model; variable-coefficient hyperbolic system
Mathematics Subject Classification: 34H05, 35L60, 93D15

1. Introduction

Freeway traffic modeling and management have been intensively investigated in recent decades. It is of great importance to reduce stop-and-go oscillations in traffic control. The traffic flow can be represented by the typical Aw-Rascle-Zhang(ARZ) model [1, 2], consisting of a set of nonlinear hyperbolic PDEs that describe the evolution of traffic density and velocity evolution.

In 1984, in the framework of the C^1 solution, the stability of homogeneous nonlinear 2×2 systems was obtained using the characteristic method in [3]. In 1999, another method was introduced: the quadratic Lyapunov function. This function was first used to analyze the exponential stability of linear hyperbolic equations in [4]. Then, it was extended to the stability analysis of a nonlinear hyperbolic system under the C^1 norms in [5], and sufficient conditions for system stability had been obtained.

Prieur et al. studied a class of hyperbolic balance law systems and proved its well-posedness under boundary feedback control; then a sufficient exponential stability condition was derived using operator theory in [6].

Also, for the hyperbolic balance law system, Wang et al. constructed a suitable Lyapunov function in [7], which led to the exponential stability of the equilibrium of the H^2 solution. This method was applied to the ARZ traffic flow equation in [8]. In [9], asymptotic spectral analysis was conducted on a 1-D 2×2 constant-coefficients linear hyperbolic equation with proportional feedback control, the spectrum determined the growth condition held, and then the exponential stability of the system was established. For the case of variable coefficients, the exponential stability of the system under the H^2 norm was obtained by constructing the weighted Lyapunov function in [10]. Hayat et al. proposed proportional-integral (PI) control and used the Lyapunov method to study the exponential stability and output regulation of closed-loop systems in [11]. In [12], the input delay compensation design of the ARZ traffic flow model based on first-order 2×2 nonlinear hyperbolic systems was studied, and the exponential stability of the closed-loop system under the L^2 norm was proved.

The most basic control objective of freeway traffic is to maintain the stability of traffic volume, speed, and density at a steady value and to suppress the oscillation as much as possible. A multi-value cellular automata model under Lagrange coordinates was proposed, and the traffic flow was simulated on the basis of the evolution equation of the model. And it is concluded that the lower the density, the more lanes there are, and the greater the traffic flow in [13].

The common control measures include on-ramp metering, which means that the vehicles entering the expressway are regulated by the traffic lights on the on-ramp, and the variable speed limits (VSL), that is, through variable message sign (VMS), which controls the speed limit of passing vehicles [14–16]. In [17], the influence of ramp metering control strategy on single-segment road traffic flow was analyzed. Based on the backstepping method, the results showed that this method reduces the stop-and-go waves in congested traffic and shortens the adjustment time. Then, in [18] and [19], the ramp metering strategy was used to design the output feedback controller to ensure that the traffic flow on the two connected roads was stable simultaneously to suppress traffic oscillations. In [20], the variable speed limit control strategy was used to design the controller combined with the backstepping transformation, and the exponential stability of the traffic flow of a single section is achieved using the Lyapunov function. For the problem of traffic congestion on a one-way, two-lane freeway, two different VSLs were applied at the exit boundary, and finally converged to the equilibrium point in finite time [21]. To the authors' knowledge, the latest research progress on the ARZ model indicates that the current control strategies for ARZ traffic flow remain ramp metering [22], variable speed limits [23], or a combination of both [24]. Zhang et al. studied a system of linear hyperbolic equations with constant coefficients, which was derived from the ARZ traffic flow model, with ramp metering and variable speed control as boundary conditions. The proportional control and PI control are designed in [24] and [25], respectively. Based on the Lyapunov function, sufficient conditions for exponential stability under the L^2 norm and sufficient conditions for parameters are obtained.

However, to the authors' knowledge, there has been limited research on the exponential stability of variable-coefficient hyperbolic systems under varying steady states concerning the spatial domain x when linearizing the ARZ model, with ramp metering and variable speed limit control serving as boundary conditions. In this paper, the exponential stability of the ARZ traffic flow model based on a 2×2 variable-coefficient hyperbolic system under proportional control is studied.

The contribution is as follows: first, considering that the steady-state values of state quantity density and speed in ARZ traffic flow are variables related to position x, combining ramp metering and variable speed limit as boundary control, a variable-coefficient one-dimensional 2×2 hyperbolic system is obtained. Second, a new Lyapunov function is chosen, where the coefficients of the Lyapunov function are constructed from the solution of a partial differential equation. It is derived that when the feedback parameters satisfy the constraint conditions, the system achieves exponential stability. Third, through numerical simulations, we concluded that the velocity value $v(L, t)$ on the right-hand side of the system converges to the steady-state value $v^*(L)$.

The outline is as follows: In Section 2, the linearized ARZ model and boundary conditions are introduced. First, the Riemann coordinate transformation is defined, and after considering that the system steady-state is variable concerning position x, we obtain a hyperbolic system of equations with variable coefficients in the free/congestion region. For congestion, a proportional feedback controller combining on-ramp metering and variable speed limits is proposed, which is rewritten as an abstract evolution equation. In Section 3, the well-posedness of the closed-loop system is proved using the operator semigroup theory and Sobolev embedding theorem. In Section 4, a strict Lyapunov function is constructed to prove the exponential stability of the system in the L^2 norm, and the stability region for the feedback gain value is given. Finally, the numerical simulation is given to illustrate the effectiveness of the developed boundary feedback control.

2. Modeling and controller design

2.1. Modeling of macroscopic traffic flow

The macroscopic traffic flow dynamics of the freeway is generally described by the ARZ model:

$$\begin{cases} \partial_t \rho + \partial_x(\rho v) = 0, \\ \partial_t v + (v - \rho p'(\rho))\partial_x v = \dfrac{V(\rho) - v}{\tau_0}, \end{cases} \tag{2.1}$$

where the state variable $\rho(x, t)$ is the density of the traffic, and $v(x, t)$ is the speed of the traffic; $(x, t) \in [0, L] \times [0, \infty)$, x and t represent the position and time, respectively, and τ_0 is the relaxation time related to driving behavior. The variable $p(\rho)$ is defined as the traffic pressure, an increasing function of density,

$$p(\rho) = v_f (\frac{\rho}{\rho_m})^\gamma, \tag{2.2}$$

and $V(\rho)$ represents the equilibrium speed curve and satisfies

$$V(\rho) = v_f - p(\rho) = v_f(1 - (\frac{\rho}{\rho_m})^\gamma), \tag{2.3}$$

where v_f is the free flow velocity, ρ_m is the maximum density, and $\gamma > 0$ is generally a constant of about 1 (see [2] and its references for a detailed description of the model).

2.2. Riemann transformation and linearization

We define new variables (w, z) in Riemann coordinates, let

$$\begin{cases} w = v + v_f(\frac{\rho}{\rho_m})^\gamma, \\ z = v. \end{cases} \tag{2.4}$$

Then the ARZ model (2.1) can be described under the Riemann coordinate as

$$\begin{cases} \partial_t w + z\partial_x w = \frac{v_f - w}{\tau_0}, \\ \partial_t z + [(1+\gamma)z - \gamma w]\partial_x z = \frac{v_f - w}{\tau_0}. \end{cases} \tag{2.5}$$

To obtain the linearized ARZ model, assume $(\rho^*(x), v^*(x))$ and $(w^*(x), z^*(x))$ are respectively steady states of system (2.1) and system (2.4), and satisfy $z^*(x) = v^*(x)$, $w^*(x) = v^*(x) + v_f(\frac{\rho^*(x)}{\rho_m})^\gamma$. Furthermore, $(w^*(x), z^*(x))$ satisfy the system (2.5) such that we have

$$\begin{cases} z^*(x)\partial_x w^*(x) = \frac{v_f - w^*(x)}{\tau_0}, \\ [(1+\gamma)z^*(x) - \gamma w^*(x)]\partial_x z^*(x) = \frac{v_f - w^*(x)}{\tau_0}. \end{cases} \tag{2.6}$$

Define the deviations of the state (w, z) with respect to the steady state $(w^*(x), z^*(x))$ as:

$$\begin{cases} \tilde{w} = w - w^*(x), \\ \tilde{z} = z - z^*(x), \end{cases} \tag{2.7}$$

therefore, the linearized ARZ model can be obtained from a 2×2 hyperbolic system with variable coefficients:

$$\begin{cases} \partial_t \tilde{w} + \lambda_1(x)\partial_x \tilde{w} + \delta\tilde{w} = 0, \\ \partial_t \tilde{z} - \lambda_2(x)\partial_x \tilde{z} + \delta\tilde{w} = 0, \end{cases} \tag{2.8}$$

where

$$\lambda_1(x) = z^*(x) = v^*(x) > 0, \;\; \lambda_2(x) = -(1+\gamma)z^*(x) + \gamma w^*(x), \;\; \delta = \frac{1}{\tau_0} > 0. \tag{2.9}$$

Moreover, by (2.4) and (2.9), it has

$$\lambda_2(x) = -(1+\gamma)z^*(x) + \gamma w^*(x) = -v^*(x) + \gamma v_f(\frac{\rho^*(x)}{\rho_m})^\gamma. \tag{2.10}$$

It is obvious that $\lambda_2(x)$ can be positive or negative. Therefore, the speed-density relationship diagram can be divided into two parts:

Free-flow regime: $\lambda_2(x) < 0$, that is, $v^*(x) > \gamma v_f(\frac{\rho^*(x)}{\rho_m})^\gamma$. The speed information of the linearized ARZ model of (2.8) is transmitted from the left boundary $x = 0$ to the right boundary $x = L$.

Congested regime: $\lambda_2(x) > 0$, that is, $v^*(x) < \gamma v_f(\frac{\rho^*(x)}{\rho_m})^\gamma$. The speed information of the linearized ARZ model of (2.8) is transmitted from the right boundary $x = L$ to the left boundary $x = 0$. So, the hetero-directional propagations of traffic flow might lead to the shock waves of stop-and-go traffic.

In this paper, we focus on the controller design for the congested regime.

2.3. Design of proportional feedback controller

To regulate freeway traffic, we designed the on-ramp metering controller $r(t)$ and the variable speed limit controller $v(L,t)$, based on the regimes in which traffic lies, as shown in Figure 1.

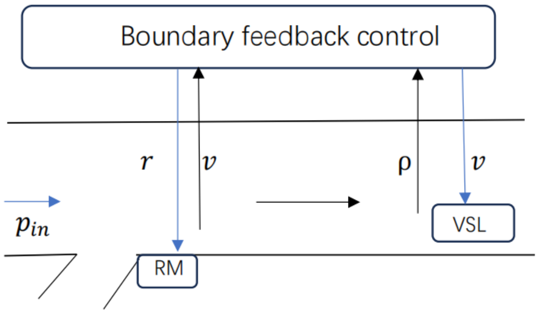

Figure 1. Boundary control strategies of freeway traffic flow under congestion.

On-ramp metering: we should regulate the upstream on-ramp flow rate $r(t)$ based on the measurements collected from the downstream boundary $x = L$:

$$r(t) = r^* + k_\rho(\rho(L,t) - \rho^*(L)). \tag{2.11}$$

Variable speed limit: As the traffic lies in the congestion regime, the characteristic velocity of speed propagating is from downstream to upstream, we should regulate the downstream speed $v(L,t)$ based on the measurement $v(0,t)$ at the upstream boundary, i.e.,

$$v(L,t) = v^*(L) + k^v(v(0,t) - v^*(0)), \tag{2.12}$$

where k^ρ, k^v are the feedback gains, and $r*$ is the normal regulation rate of the on-ramp.

Let $\tilde{\rho} = \rho - \rho^*(x)$, $\tilde{v} = v - v^*(x)$; then (2.11) and (2.12) become

$$\begin{cases} r(t) = r^* + k_\rho\tilde{\rho}(L,t), \\ \tilde{v}(L,t) = k_v\tilde{v}(0,t). \end{cases} \tag{2.13}$$

Assume that the conservation conditions satisfied by the traffic flow at the upstream entrance boundary and the conservation conditions at the steady state of the traffic flow are, respectively,

$$p_{in} + r(t) = \rho(0,t)v(0,t), \tag{2.14}$$

$$p_{in} + r^* = \rho^*(0)v^*(0), \tag{2.15}$$

where p_{in} is the traffic demand of the mainline.

Combining (2.13)–(2.15), we have

$$k_\rho\tilde{\rho}(L,t) = \rho(0,t)v(0,t) - \rho^*(0)v^*(0),$$

and linearizing by the first-order Taylor formula of a binary function, we have the following linearized boundary condition:

$$k_\rho\tilde{\rho}(L,t) = v^*(0)\tilde{\rho}(0,t) + \rho^*(0)\tilde{v}(0,t). \tag{2.16}$$

Furthermore, assume that $\gamma = 1$ and let $\alpha = \frac{v_f}{\rho_m}$; we could rewrite the boundary conditions for system (2.8) in the Riemann coordinates as:

$$\begin{aligned}\tilde{w}(0,t) =&\tilde{v}(0,t) + \alpha\tilde{\rho}(0,t)\\ =&(1 - \frac{\alpha\rho^*(0)}{v^*(0)})\tilde{v}(0,t) + \frac{\alpha k_\rho}{v^*(0)}\tilde{\rho}(L,t)\\ =&\frac{k_\rho}{v^*(0)}\tilde{w}(L,t) + (1 - \frac{\alpha\rho^*(0)}{v^*(0)} - \frac{k_\rho k_v}{v^*(0)})\tilde{z}(0,t)\\ =&k_1\tilde{w}(L,t) + k_2\tilde{z}(0,t),\end{aligned} \tag{2.17}$$

and

$$\tilde{z}(L,t) = k_3\tilde{z}(0,t), \tag{2.18}$$

where

$$k_1 = \frac{k_\rho}{v^*(0)}, \quad k_2 = 1 - \frac{\alpha\rho^*(0)}{v^*(0)} - \frac{k_\rho k_v}{v^*(0)}, \quad k_3 = k_v. \tag{2.19}$$

Therefore, we have a PDE system under a proportional controller

$$\begin{cases}\partial_t\tilde{w} + \lambda_1(x)\partial_x\tilde{w} + \delta\tilde{w} = 0,\\ \partial_t\tilde{z} - \lambda_2(x)\partial_x\tilde{z} + \delta\tilde{w} = 0,\\ \tilde{w}(0,t) = k_1\tilde{w}(L,t) + k_2\tilde{z}(0,t),\\ \tilde{z}(L,t) = k_3\tilde{z}(0,t).\end{cases} \tag{2.20}$$

Without loss of generality, let $L = 1$ for convenience. Assume that the Hilbert state space

$$\mathcal{H} = L^2(0,1) \times L^2(0,1), \tag{2.21}$$

equipped with the following inner product

$$\langle X_1, X_2\rangle = \int_0^1 [f_1(x)\overline{f_2(x)} + g_1(x)\overline{g_2(x)}]\mathrm{d}x, \tag{2.22}$$

where $X_i = (f_i, g_i) \in \mathcal{H}(i = 1,2)$, and $\bar{f}$ is the conjugate of f. Moreover, the norm of X_i is induced by the inner product

$$\| X_i \|^2 = \int_0^1 [\,|f_i(x)|^2 + |g_i(x)|^2\,]\mathrm{d}x, \quad i = 1,2. \tag{2.23}$$

Define linear operator $\mathcal{A}: D(\mathcal{A}) \subseteq \mathcal{H} \to \mathcal{H}$ by

$$\mathcal{A}X = \begin{pmatrix} -\lambda_1(x)\frac{\partial}{\partial x} - \delta & 0\\ -\delta & \lambda_2(x)\frac{\partial}{\partial x}\end{pmatrix}\begin{pmatrix} f\\ g\end{pmatrix}, \tag{2.24}$$

$$D(\mathcal{A}) = \left\{(f,g) \in (H^1(0,1))^2 \mid f(0) = k_1 f(1) + k_2 g(0), g(1) = k_3 g(0)\right\}. \tag{2.25}$$

Then system (2.20) can be written as an abstract evolution equation in $\mathcal{H}$

$$\begin{cases}\dot{X}(t) = \mathcal{A}X(t),\ t > 0,\\ X(0) = X_0,\end{cases} \tag{2.26}$$

where $X(t) = (w(\cdot,t),\ z(\cdot,t))$.

3. Well-posedness of system (2.20)

Theorem 3.1. *Let $\mathcal{A}$ be given by* (2.24) *and* (2.25). *Then $\mathcal{A}^{-1}$ exists and is compact, if the feedback parameters k_1, k_2, and k_3 satisfy*

$$(k_3-1)(1-k_1e^{-\int_0^1 \frac{\delta}{\lambda_1(s)}\mathrm{d}s})-k_2\int_0^1 \frac{\delta}{\lambda_2(s)}e^{-\int_0^s \frac{\delta}{\lambda_1(\sigma)}\mathrm{d}\sigma}\mathrm{d}s \neq 0.$$

Hence, $\sigma(\mathcal{A})$, the spectrum of $\mathcal{A}$, consists of isolated eigenvalues of finite algebraic multiplicity only.

Proof. For $X_1=(f_1,g_1)\in\mathcal{H}$, solve

$$\mathcal{A}X=X_1,\ X=(f,g)\in D(\mathcal{A}), \tag{3.1}$$

we can obtain

$$\mathcal{A}\begin{pmatrix} f \\ g\end{pmatrix}=\begin{pmatrix} -\lambda_1(x)f'-\delta f \\ \lambda_2(x)g'-\delta f\end{pmatrix}=\begin{pmatrix} f_1 \\ g_1\end{pmatrix}, \tag{3.2}$$

i.e.,

$$\begin{cases}\lambda_1(x)f'+\delta f+f_1=0,\\ \lambda_2(x)g'-\delta f-g_1=0,\\ f(0)=k_1f(1)+k_2g(0),\\ g(1)=k_3g(0).\end{cases} \tag{3.3}$$

Solving the first differential equation of (3.3), we have

$$f(x)=e^{-\int_0^x \frac{\delta}{\lambda_1(s)}\mathrm{d}s}\left[-\int_0^x \frac{f_1(s)}{\lambda_1(s)}e^{\int_0^s \frac{\delta}{\lambda_1(\sigma)}\mathrm{d}\sigma}\mathrm{d}s+f(0)\right]. \tag{3.4}$$

Let $F(x)=-e^{-\int_0^x \frac{\delta}{\lambda_1(s)}\mathrm{d}s}\int_0^x \frac{f_1(s)}{\lambda_1(s)}e^{\int_0^s \frac{\delta}{\lambda_1(\sigma)}\mathrm{d}\sigma}\mathrm{d}s$, we can get

$$f(x)=F(x)+e^{-\int_0^x \frac{\delta}{\lambda_1(s)}\mathrm{d}s}f(0). \tag{3.5}$$

Combining with the second equation of (3.3), we have

$$g'(x)=\frac{\delta}{\lambda_2(x)}f(x)+\frac{g_1(x)}{\lambda_2(x)}. \tag{3.6}$$

Integrating both sides of (3.6) yields the following

$$\begin{aligned} g(x)&=g(0)+\int_0^x \frac{\delta}{\lambda_2(s)}f(s)\mathrm{d}s+\int_0^x \frac{g_1(s)}{\lambda_2(s)}\mathrm{d}s\\ &=g(0)+\int_0^x \frac{\delta}{\lambda_2(s)}[F(s)+e^{-\int_0^s \frac{\delta}{\lambda_1(\sigma)}\mathrm{d}\sigma}f(0)]\mathrm{d}s+\int_0^x \frac{g_1(s)}{\lambda_2(s)}\mathrm{d}s\\ &=g(0)+\int_0^x \frac{\delta}{\lambda_2(s)}F(s)\mathrm{d}s+f(0)\int_0^x \frac{\delta}{\lambda_2(s)}e^{-\int_0^s \frac{\delta}{\lambda_1(\sigma)}\mathrm{d}\sigma}\mathrm{d}s+\int_0^x \frac{g_1(s)}{\lambda_2(s)}\mathrm{d}s.\end{aligned} \tag{3.7}$$

According to the third equation of (3.3), (3.5), and (3.7), we have

$$(1 - k_1 e^{-\int_0^1 \frac{\delta}{\lambda_1(s)}\mathrm{d}s}) f(0) = k_2 g(0) + k_1 F(1). \tag{3.8}$$

Similarly, according to the fourth equation of (3.3), (3.5), and (3.7), we have

$$\int_0^1 \frac{\delta}{\lambda_2(s)} e^{-\int_0^s \frac{\delta}{\lambda_1(\sigma)}\mathrm{d}\sigma}\mathrm{d}s f(0) = (k_3 - 1) g(0) - \int_0^1 \frac{\delta}{\lambda_2(s)} F(s)\mathrm{d}s - \int_0^1 \frac{g_1(s)}{\lambda_2(s)}\mathrm{d}s. \tag{3.9}$$

Combining (3.8) and (3.9), we obtain

$$\begin{aligned} &((k_3 - 1)(1 - k_1 e^{-\int_0^1 \frac{\delta}{\lambda_1(s)}\mathrm{d}s}) - k_2 \int_0^1 \frac{\delta}{\lambda_2(s)} e^{-\int_0^s \frac{\delta}{\lambda_1(\sigma)}\mathrm{d}\sigma}\mathrm{d}s) f(0) \\ &= k_1(k_3 - 1)F(1) + k_2[\int_0^1 \frac{\delta}{\lambda_2(s)} F(s)\mathrm{d}s + \int_0^1 \frac{g_1(s)}{\lambda_2(s)}\mathrm{d}s]. \end{aligned} \tag{3.10}$$

Let

$$\begin{cases} M_1 = k_1(k_3 - 1)F(1) + k_2[\int_0^1 \frac{\delta}{\lambda_2(s)} F(s)\mathrm{d}s + \int_0^1 \frac{g_1(s)}{\lambda_2(s)}\mathrm{d}s], \\ M_2 = (k_3 - 1)(1 - k_1 e^{-\int_0^1 \frac{\delta}{\lambda_1(s)}\mathrm{d}s}) - k_2 \int_0^1 \frac{\delta}{\lambda_2(s)} e^{-\int_0^s \frac{\delta}{\lambda_1(\sigma)}\mathrm{d}\sigma}\mathrm{d}s, \end{cases} \tag{3.11}$$

where $M_2 \neq 0$. We can obtain $f(0) = \frac{M_1}{M_2}$, $g(0) = \frac{1}{k_2}\frac{M_1}{M_2} - \frac{k_1}{k_2} f(1)$. So, we have the expressions of $f(x)$ and $g(x)$:

$$\begin{cases} f(x) = -e^{-\int_0^x \frac{\delta}{\lambda_1(s)}\mathrm{d}s} \int_0^x \frac{f_1(s)}{\lambda_1(s)} e^{\int_0^s \frac{\delta}{\lambda_1(\sigma)}\mathrm{d}\sigma}\mathrm{d}s + \frac{M_1}{M_2} e^{-\int_0^x \frac{\delta}{\lambda_1(s)}\mathrm{d}s}, \\ g(x) = \frac{1}{k_2}\frac{M_1}{M_2} - \frac{k_1}{k_2} f(1) + \int_0^x \frac{\delta}{\lambda_2(s)} f(s)\mathrm{d}s + \int_0^x \frac{g_1(s)}{\lambda_2(s)}\mathrm{d}s. \end{cases} \tag{3.12}$$

Hence, $\mathcal{A}^{-1}$ exists and is compact by the Sobolev embedding theorem. Therefore, $\sigma(\mathcal{A})$ consists only of isolated eigenvalues of finite algebraic multiplicity. □

4. Exponential stability of system (2.20)

In this section, we focus on constructing an appropriate Lyapunov function to analyze the exponential stability of system (2.20).

Definition 4.1. *The closed-loop system* (2.20) *is exponentially stable (in L^2 norm) if there exist $\vartheta > 0$ and $C > 0$ such that, for every initial condition $(\tilde{w}^0(x), \tilde{z}^0(x)) \in L^2((0, L); \mathbb{R}^2)$, the system solution to the Cauchy problem* (2.20) *satisfies*

$$\|\tilde{w}(\cdot, t), \tilde{z}(\cdot, t)\|_{L^2((0,L);\mathbb{R}^2)} \leq C e^{-\vartheta t} \|\tilde{w}^0, \tilde{z}^0\|_{L^2((0,L);\mathbb{R}^2)}.$$

Lemma 4.2. *The function $\eta(x)$ defined by*

$$\eta(x) = \frac{1}{-\int_0^x \frac{\delta}{\lambda_2(s)}\mathrm{d}s + 1 + \int_0^1 \frac{\delta}{\lambda_2(s)}\mathrm{d}s} \tag{4.1}$$

is a solution of the differential equation

$$\eta'(x) = \frac{\delta}{\lambda_2(x)} \eta^2(x), \tag{4.2}$$

where $\lambda_2(x)$, δ are given by (2.9)*, respectively.*

Remark 1. *It is obvious that the function* $\eta(x)$ *satisfies* $\eta(x) > 0,\ \eta'(x) > 0,\ \forall\ x \in [0,1]$*, and* $\eta(x)$ *is bounded on* $[0,1]$.

Theorem 4.3. *The nonlinear ARZ systems* (2.1)*,* (2.11)*, and* (2.12) *are exponentially stable for the* L^2*-norm provided that the boundary conditions satisfy*

$$k_1^2 \le \frac{1}{2b}, \quad 2k_2^2 b + k_3^2 \le \frac{1}{b}, \tag{4.3}$$

where k_1, k_2*, and* k_3 *are feedback parameters,*

$$b = 1 + \int_0^1 \frac{\delta}{\lambda_2(s)} \mathrm{d}s. \tag{4.4}$$

Proof. We construct the following candidate Lyapunov function:

$$V(t) = \int_0^1 [p_1(x)\tilde{w}^2(x,t) + p_2(x)\tilde{z}^2(x,t)]\mathrm{d}x, \tag{4.5}$$

where functions $p_1(x) \in C^1([0,L];(0,+\infty))$ and $p_2(x) \in C^1([0,L];(0,+\infty))$ are to be determined. Along the solution of (2.20), combining the integral formula of the distribution, the derivative of time of $V(t)$ can be obtained:

$$\begin{aligned}
\dot{V}(t) =& 2\int_0^1 [p_1(x)\tilde{w}\partial_t\tilde{w} + p_2(x)\tilde{z}\partial_t\tilde{z}]\mathrm{d}x \\
=& 2\int_0^1 [p_1(x)(-\lambda_1(x)\partial_x\tilde{w} - \delta\tilde{w})\tilde{w} + p_2(x)(\lambda_2(x)\partial_x\tilde{z} - \delta\tilde{w})\tilde{z}]\mathrm{d}x \\
=& 2\int_0^1 [-p_1(x)\lambda_1(x)\tilde{w}\partial_x\tilde{w} + p_2(x)\lambda_2(x)\tilde{z}\partial_x\tilde{z}]\mathrm{d}x - 2\int_0^1 [\delta p_1(x)\tilde{w}^2 + \delta p_2(x)\tilde{w}\tilde{z}]\mathrm{d}x \\
=& -\int_0^1 p_1(x)\lambda_1(x)\mathrm{d}\tilde{w}^2 + \int_0^1 p_2(x)\lambda_2(x)\mathrm{d}\tilde{z}^2 - 2\int_0^1 [\delta p_1(x)\tilde{w}^2 + \delta p_2(x)\tilde{w}\tilde{z}]\mathrm{d}x \\
=& -p_1(1)\lambda_1(1)\tilde{w}^2(1,t) + p_2(1)\lambda_2(1)\tilde{z}^2(1,t) + p_1(0)\lambda_1(0)\tilde{w}^2(0,t) - p_2(0)\lambda_2(0)\tilde{z}^2(0,t) \\
&+ \int_0^1 (p_1(x)\lambda_1(x))_x\tilde{w}^2\mathrm{d}x - \int_0^1 (p_2(x)\lambda_2(x))_x\tilde{z}^2\mathrm{d}x - 2\int_0^1 [\delta p_1(x)\tilde{w}^2 + \delta p_2(x)\tilde{w}\tilde{z}]\mathrm{d}x \\
\doteq& -V_1 - V_2,
\end{aligned} \tag{4.6}$$

where

$$V_1 = \int_0^1 (\tilde{w},\tilde{z})\Lambda\begin{pmatrix}\tilde{w}\\ \tilde{z}\end{pmatrix}\mathrm{d}x, \quad \Lambda = \begin{pmatrix} -(p_1(x)\lambda_1(x))_x + 2\delta p_1(x) & \delta p_2(x) \\ \delta p_2(x) & p_2(x)\lambda_2(x)\end{pmatrix}, \tag{4.7}$$

$$V_2 = p_1(1)\lambda_1(1)\tilde{w}^2(1,t) - p_2(1)\lambda_2(1)\tilde{z}^2(1,t) - p_1(0)\lambda_1(0)\tilde{w}^2(0,t) + p_2(0)\lambda_2(0)\tilde{z}^2(0,t). \tag{4.8}$$

It is obvious that the exponential stability is guaranteed if V_1 and V_2 are positive definite quadratic forms.

For $\forall x \in [0,1]$, we assume

$$p_1(x) = \frac{1}{\lambda_1(x)\eta(x)}, \quad p_2(x) = \frac{\eta(x)}{\lambda_2(x)}. \tag{4.9}$$

It is easy to verify that

$$\begin{aligned} &-(p_1(x)\lambda_1(x))_x + 2\delta p_1(x) = \frac{\eta'(x)}{\eta^2(x)} + \frac{2\delta}{\lambda_1(x)\eta(x)} > 0, \quad (p_2(x)\lambda_2(x))_x = \eta'(x) > 0, \\ &[-(p_1(x)\lambda_1(x))_x + 2\delta p_1(x)](p_2(x)\lambda_2(x))_x - \delta^2 p_2^2(x) = 2\delta \frac{\eta'(x)}{\lambda_1(x)\eta(x)} > 0. \end{aligned} \tag{4.10}$$

Then in this case, by continuity, V_1 is positive.

Next, we consider the boundary term V_2. Substituting the boundary conditions $\tilde{w}(0,t) = k_1\tilde{w}(1,t) + k_2\tilde{z}(0,t), \quad \tilde{z}(1,t) = k_3\tilde{z}(0,t)$ into V_2, we have

$$\begin{aligned} V_2 =& \Big(p_1(1)\lambda_1(1) - 2k_1^2 p_1(0)\lambda_1(0)\Big)\tilde{w}^2(1,t) \\ &+ \Big(p_2(0)\lambda_2(0) - k_3^2 p_2(1)\lambda_2(1) - 2k_2^2 p_1(0)\lambda_1(0)\Big)\tilde{z}^2(0,t) \\ =& \Big(\frac{1}{\eta(1)} - 2k_1^2\frac{1}{\eta(0)}\Big)\tilde{w}^2(1,t) + \Big(\eta(0) - k_3^2\eta(1) - 2k_2^2\frac{1}{\eta(0)}\Big)\tilde{z}^2(0,t) \\ =& \Big(1 - 2(1 + \int_0^1 \frac{\delta}{\lambda_2(s)}\mathrm{d}s)k_1^2\Big)\tilde{w}^2(1,t) + \Big(\frac{1}{1 + \int_0^1 \frac{\delta}{\lambda_2(s)}\mathrm{d}s} - k_3^2 - 2(1 + \int_0^1 \frac{\delta}{\lambda_2(s)}\mathrm{d}s)k_2^2\Big)\tilde{z}^2(0,t) \\ =& (1 - 2bk_1^2)\tilde{w}^2(1,t) + (\frac{1}{b} - k_3^2 - 2bk_2^2)\tilde{z}^2(0,t), \end{aligned} \tag{4.11}$$

where b is defined in (4.4). If the system parameters satisfy condition (4.3), we have $V_2 > 0$.

Therefore, there must exist a positive constant c such that $\dot{V}(t) < -cV(t)$. □

Remark 2. *Combining Eq* (2.19)*, it can be concluded that when the feedback gains k_ρ and k_v in controllers* (2.11) *and* (2.12) *satisfy the following conditions, the nonlinear ARZ systems* (2.1)*,* (2.11)*, and* (2.12) *are exponentially stable for the L^2-norm*

$$k_\rho^2 \le \frac{v^{*2}(0)}{2b}, \quad 2(\beta - \frac{k_\rho k_v}{v^*(0)})^2 b + k_v^2 \le \frac{1}{b}, \tag{4.12}$$

where b is defined in (4.4)*, $\beta = 1 - \frac{\alpha\rho^*(0)}{v^*(0)}$.*

5. Simulation

In this section, we illustrate Theorem 4.3 using MATLAB numerical simulations. Without loss of generality and for computational convenience. The road parameters are shown in Table 1.

Table 1. Road traffic parameters.

Road length	Relaxation time	Maximum density	Free flow velocity
$L = 1km$	$\tau_0 = \frac{1}{20}h$	$\rho_m = 150Vehicle/km$	$v_f = 150km/h$

The steady-state is chosen with initial conditions prescribed as $v^*(0) = 60km/h$, $\rho^*(0) = 90Vehicle/km$, and the non-uniform steady-state is $v^*(x) = 60 + 5x$, $\rho^*(x) = 90 - 10x$. Based on Table 1, the initial steady-state and the constraint condition (4.3) of Theorem 4.3, we can obtain the values of the control parameters as follows: $k_1 = -0.5$, $k_2 = 0.3$, $k_3 = 0.4$. Combined with equation (4.11), we take the feedback gain $k_\rho = -30$, $k_v = 0.4$.

In Figure 2, Figures 2(a) and 2(b) respectively represent the changes of disturbance state variables $\tilde{w}$ and $\tilde{z}$ over time and space, where the initial conditions are $\tilde{w}(x, 0) = \cos(2\pi x) + 2\sin(2\pi x)$ and $\tilde{z}(x, 0) = 5\cos(2\pi x) + \sin(2\pi x) - 3x$. It is evident from Figure 2(a) that the state variable $\tilde{w}$ exhibits significant fluctuations above and below zero at the initial moment but eventually converges to zero. Similarly, Figure 2(b) shows that the state variable $\tilde{z}$ also initially exhibits significant fluctuations above and below zero but similarly converges to zero. Figure 3 shows that the velocity value $v(L, t)$ at the right boundary (represented by the red line) experiences large fluctuations at the initial moment but ultimately converges to its steady-state value $v^*(L)$ (represented by the blue line).

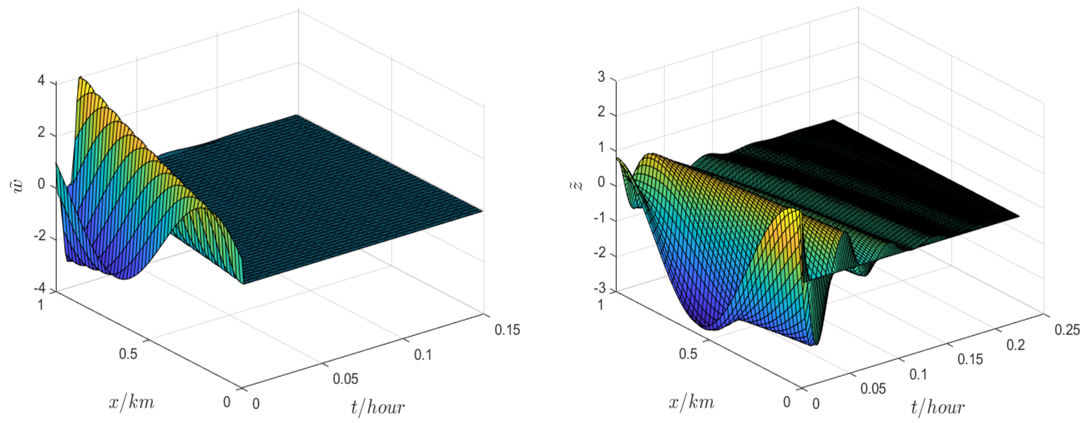

(a) Convergence of the state $\tilde{w}(x, t)$ (b) Convergence of the state $\tilde{z}(x, t)$

Figure 2. The evolution process of the state $\tilde{w}(x, t), \tilde{z}(x, t)$ of the system (2.20) with respect to time and space.

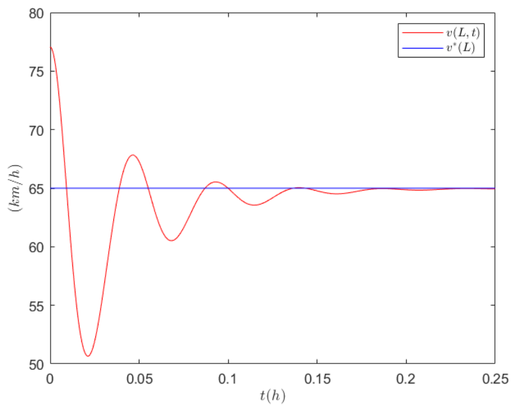

Figure 3. Convergence of $v(L, t)$ at $x = L$ to the value $v^*(L)$.

6. Conclusions

This paper considers the stability of the linearized variable-coefficient ARZ equation with boundary control. The proportional boundary feedback controller that combined ramp metering and variable speed limits was designed to regulate stop-and-go traffic flow oscillations caused by congestion. Constructing a suitable Lyapunov function, it has been proven that the system is exponentially stable when the feedback parameters satisfy certain constraints. Numerical simulations demonstrate the effectiveness of the proposed boundary control and the feasibility of the selected parameters. In future work, we attempt to study the eigenvalue problem $\mathcal{A}X = \mu X$ and obtain the distribution of eigenvalues. The spectrum-determined growth condition and Riesz basis property are also of interest.

Author contributions

All authors contributed equally to this work. All authors have read and approved the final version of the manuscript for publication.

Use of Generative-AI tools declaration

The authors declare that they have not used Artificial Intelligence (AI) tools in the creation of this article.

Acknowledgments

This work was supported by the National Natural Science Foundation of China under Grant No.12001343.

Conflict of interest

The authors declare that they have no conflict of interest.

References

1. A. Aw, M. Rascle, Resurrection of "second order" models of traffic flow, *SIAM J. Appl. Math.*, **60** (2000), 916–938. https://doi.org/10.1137/S0036139997332099
2. H. M. Zhang, A non–equilibrium traffic model devoid of gas-like behavior, *Transport. Res. B-Meth.*, **36** (2002), 275–290. https://doi.org/10.1016/S0191-2615(00)00050-3
3. J. M. Greenberg, L. T. Tsien, The effect of boundary damping for the quasilinear wave equation, *J. Differ. Equ.*, **52** (1984), 66–75. https://doi.org/10.1016/0022-0396(84)90135-9
4. J. M. Coron, B. d'Andréa-Novel, G. Bastia, A Lyapunov approach to control irrigation canals modeled by Saint-Venant equations, In: *1999 European Control Conference*, 1999, 3178–3183. https://doi.org/10.23919/ECC.1999.7099816

5. H. Zhao, J. Zhan, L. Zhang, Saturated boundary feedback stabilization for LWR traffic flow model, *Syst. Control Lett.*, **173** (2023), 105465. https://doi.org/10.1016/j.sysconle.2023.105465
6. C. Prieur, J. J. Winkin, Boundary feedback control of linear hyperbolic systems: Application to the Saint-Venant-Exner equations, *Automatica*, **89** (2018), 44–51. https://doi.org/10.1016/j.automatica.2017.11.028
7. K. Wang, Z. Wang, W. Yao, Boundary feedback stabilization of quasilinear hyperbolic systems with partially dissipative structure, *Syst. Control Lett.*, **146** (2020), 104815. https://doi.org/10.1016/j.sysconle.2020.104815
8. L. Zhang, C. Prieur, J. Qiao, Local proportional-integral boundary feedback stabilization for quasilinear hyperbolic systems of balance laws, *SIAM J. Control Optim.*, **58** (2020), 2143–2170. https://doi.org/10.1137/18M1214883
9. D. Zhao, D. Fan, Y. Guo, The spectral analysis and exponential stability of a 1-d 2×2 Hyperbolic system with proportional feedback control, *Int. J. Control, Autom. Syst.*, **20** (2022), 2633–2640. http://dx.doi.org/10.1007/s12555-021-0507-0
10. A. Hayat, P. Shang, A quadratic Lyapunov function for Saint-Venant equations with arbitrary friction and space varying slope, *Automatica*, **100** (2019), 52–60. https://doi.org/10.1016/j.automatica.2018.10.035
11. A. Hayat, Y. Hu, P. Shang, PI control for the cascade channels modeled by general Saint-Venant equations, *IEEE Trans. Automat. Control*, **69** (2024), 4974–4987. https://doi.org/10.1109/TAC.2023.3341767
12. J. Qi, S. Mo, M. Krstic, Delay-compensated distributed PDE control of traffic with connected/automated vehicles, *IEEE Trans. Automat. Control*, **68** (2023), 2229–2244. https://doi.org/10.1109/TAC.2022.3174032
13. J. Zeng, Y. Qian, F. Yin, L. Zhu, D. Xu, A multi-value cellular automata model for multi-lane traffic flow under lagrange coordinate, *Comput. Math. Organ. Theory*, **28** (2022), 178–192. https://doi.org/10.1007/s10588-021-09345-w
14. Z. Li, C. Xu, D. Li, W. Wang, Comparing the effects of ramp metering and variable speed limit on reducing travel time and crash risk at bottlenecks, *IET Intell. Transp. Syst.*, **12** (2018), 120–126. https://doi.org/10.1049/iet-its.2017.0064
15. J. R. D. Frejo, B. De Schutter, Logic-based traffic flow control for ramp metering and variable speed limits-Part 1: Controller, *IEEE Trans. Intell. Transp. Syst.*, **22** (2021), 2647–2657. https://doi.org/10.1109/TITS.2020.2973717
16. Z. He, L. Wang, Z. Su, W. Ma, Integrating variable speed limit and ramp metering to enhance vehicle group safety and efficiency in a mixed traffic environment, *Phys. A*, **641** (2024), 129754. https://doi.org/10.1016/j.physa.2024.129754
17. H. Yu, M. Krstic, Traffic congestion control for Aw-Rascle-Zhang model, *Automatica*, **100** (2019), 38–51. https://doi.org/10.1016/j.automatica.2018.10.040
18. H. Yu, J. Auriol, M. Krstic, Simultaneous downstream and upstream output-feedback stabilization of cascaded freeway traffic, *Automatica*, **136** (2022), 110044. https://doi.org/10.1016/j.automatica.2021.110044

19. N. Espitia, J. Auriol, H. Yu, M. Krstic, Traffic flow control on cascaded roads by event-triggered output feedback, *Int. J. Robust Nonlin.*, **32** (2022), 5919–5949. https://doi.org/10.1002/rnc.6122
20. N. Espitia, H. Yu, M. Krstic, Event-triggered varying speed limit control of stop-and-go traffic, *IFAC-PapersOnLine*, **53** (2020), 7509–7514. https://doi.org/10.1016/j.ifacol.2020.12.1343
21. H. Yu, M. Krstic, Output feedback control of two-lane traffic congestion, *Automatica*, **125** (2021), 109379. https://doi.org/10.1016/j.automatica.2020.109379
22. S. C. Vishnoi, S. A. Nugroho, A. F. Taha, C. G. Claudel, Traffic state estimation for connected vehicles using the second-order aw-rascle-zhang traffic model, *IEEE T. Intell. Transp.*, **25** (2024), 16719–16733. https://doi.org/10.1109/TITS.2024.3420438
23. P. Zhang, B. Rathnayake, M. Diagne, M. Krstic, Performance-barrier-based event-triggered boundary control of congested ARZ traffic PDEs, *IFAC-PapersOnLine*, **58** (2024), 182–187. https://doi.org/10.1016/j.ifacol.2024.07.337
24. L. Zhang, H. Luan, Y. Lu, C. Prieur, Boundary feedback stabilization of freeway traffic networks: ISS control and experiments, *IEEE Trans. Control Syst. Technol.*, **30** (2022), 997–1008. https://doi.org/10.1109/TCST.2021.3088093
25. L. Zhang, C. Prieur, J. Qiao, PI boundary control of linear hyperbolic balance laws with stabilization of ARZ traffic flow models, *Syst. Control Lett.*, **123** (2019), 85–91. https://doi.org/10.1016/j.sysconle.2018.11.005